

THERMAL STABILITY AND EXTRA-STRENGTH OF AN ULTRAFINE GRAINED STAINLESS STEEL PRODUCED BY HIGH PRESSURE TORSION

M.M. Abramova¹, N.A. Enikeev^{1,3}, X. Sauvage², A. Etienne², B. Radiguet²,
E. Ubyivovk³ and R.Z. Valiev^{1,3}

¹Institute of Physics of Advanced Materials, Ufa State Aviation Technical University, Russia

²University of Rouen, Groupe de Physique des Matériaux, CNRS (UMR 6634), France

³Saint Petersburg State University, St. Petersburg, Russia

Received: September 30, 2015

Abstract. Investigations of an ultrafine-grained (UFG) Cr-Ni austenitic stainless steel produced by high pressure torsion (HPT) at room and elevated (400 °C) temperatures followed by series of annealing up to 700 °C are reported. The grain size of the alloy processed at room temperature (55 nm) was found to be about twice lower than the grain size of the alloy (90 nm) processed at elevated temperature. Besides, both as-processed states demonstrated a very high value of microhardness (~590 Hv), while the steel in initial quenched state had the microhardness about 155 Hv. It is shown that the hardness of the steel in both UFG states does not decrease with annealing up to 650 °C, and even a certain increase in hardness was observed for the steel produced at room temperature. At higher temperature (700 °C), the recrystallization starts, and precipitation was observed.

1. INTRODUCTION

An increasing interest is being paid nowadays to ultrafine grained (UFG) and nanostructured materials thanks to their high strength and enhanced functional properties [1,2]. It is well-known [3-5] that severe plastic deformation (SPD) techniques are capable of significant enhancement of mechanical properties thanks to unique microstructures characterized by ultrafine grains and specific nanostructural features as precipitations, nanotwins, elevated defect densities and so on [6]. These features can contribute to additional hardening contributions in nanostructured materials, thus leading to further increase of their strength. Recently, it was found that SPD induced grain boundary segregations can form in austenitic stainless steels during processing at elevated temperature and after additional annealing [7,8] but not at room temperature. It is important to note that such segregations may

lead to additional hardening of UFG materials [7]. However, it is matter of question how stable could be the achieved level of mechanical properties during thermal treatment. Some authors reported on additional increase of strength after annealing of an UFG austenitic stainless steel produced by high pressure torsion (HPT) at room temperature [8,9]. The strength reached its maximum after annealing at ~550 °C, where grain boundary segregations were formed. The level of as-processed material strength kept being stable until ~600 °C [8], thus, revealing an outstanding thermal stability of the UFG structures formed by SPD.

This paper is devoted to the investigation of the thermal stability of an UFG Cr-Ni (SS 316) austenitic steel produced by HPT at room and elevated (400 °C) temperatures. Changes in microstructure and corresponding hardness level with annealing are measured and discussed in terms of thermal stability of the nanostructural features.

Corresponding author: M.M. Abramova, e-mail: abramovamm@yandex.ru

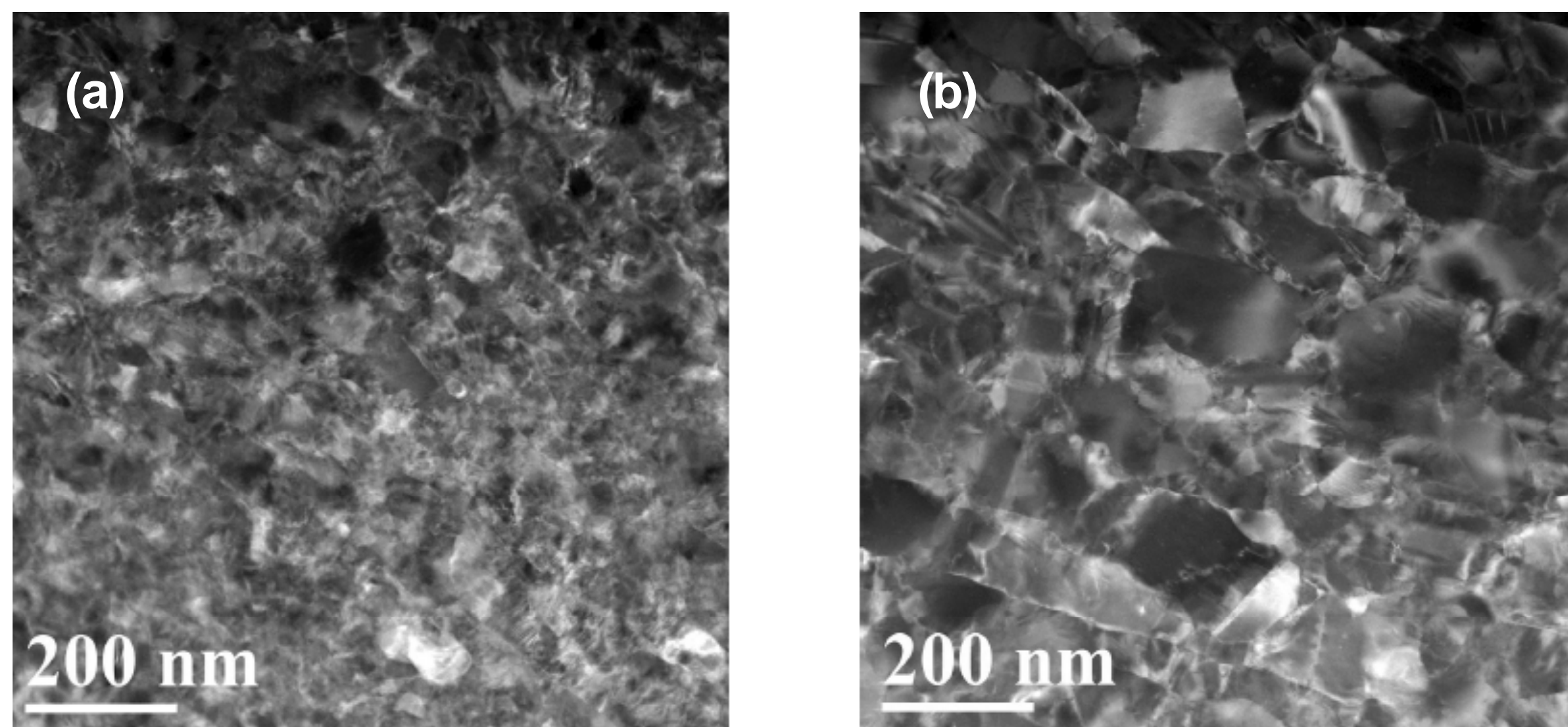


Fig. 1. STEM dark field images of the microstructure of the UFG steel produced by HPT at (a) – room temperature, (b) – $T = 400\text{ }^{\circ}\text{C}$.

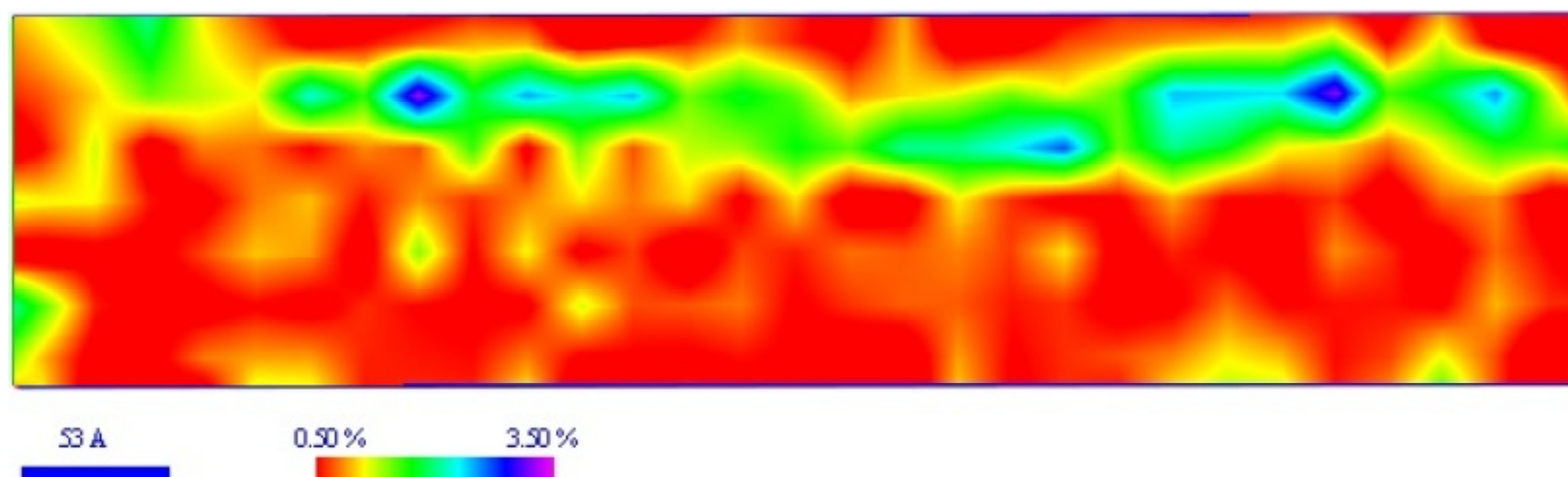


Fig. 2. 2-D map of Si GB segregations in an UFG austenitic stainless steel produced by HPT at $400\text{ }^{\circ}\text{C}$.

2. EXPERIMENTAL PROCEDURE

An austenitic Cr-Ni stainless steel (Fe – 0.05C – 0.7Si – 1.1Mn – 17.1Cr – 10.6Ni – 0.24Cu – 2.25Mo – 0.027P, wt.%) was the object of the present study. Prior to SPD processing the steel specimens were annealed at $1050\text{ }^{\circ}\text{C}$ for an hour and then water quenched. The steel was nanostructured by HPT at room temperature and at $400\text{ }^{\circ}\text{C}$, the pressure was 6 GPa, the number of HPT turns $n=10$. The produced UFG specimens were in the form of the discs of 20 mm in diameter and with thickness ~ 1 mm. All studies were carried out on middle of the radius of samples. The microstructure investigations were conducted by scanning transmission electron microscopy (STEM) Zeiss Libra 200FE (Research Park of St. Petersburg State University at the Nanotechnology Center) and JEOL ARM200F (Groupe de Physique des Matériaux, University of Rouen) operated at 200 kV. The average grain size was calculated using TEM dark field images from half-radius of the disc normal section with the help of mean intersect lengths over 300 grains for each state. Atom probe tomography (APT) analyses [10] were carried out in Cameca FlexTAP with Field evaporation pulses provided by femtosecond UV laser at 50K. The samples for APT were prepared by electropolishing as thin tips with a radius of about 20-50 nm. The microhardness measurements were

carried out using a microhardness tester Micromet with a load of 0.1 kg.

3. RESULTS AND DISCUSSION

In the initial quenched state, the microstructure was characterized by fully austenitic grains with an average size of $25\text{ }\mu\text{m}$. The hardness of the initial material was estimated as 155 ± 11 Hv. After HPT at room temperature an UFG microstructure was formed with a grain size of ~ 55 nm (Fig. 1a) and in this state the dislocation density was measured up to $\sim 10^{15}\text{ m}^{-2}$ [7]. After HPT at $400\text{ }^{\circ}\text{C}$ the UFG structure exhibits austenitic grains with the size ~ 90 nm in short dimension. Grains had an elongated shape, with the shape factor of ~ 2 (Fig. 1b); while the dislocation density was estimated up to $\sim 0.6\times 10^{15}\text{ m}^{-2}$ [7]. Also a small fraction ($\sim 7\%$) of twinned grains was observed in the UFG steel produced by HPT at $400\text{ }^{\circ}\text{C}$. Another striking difference between the states concerned the state of their grain boundaries. Fig. 2 shows 2D map of distribution of Si atoms along a grain boundary in the UFG steel produced by HPT at $400\text{ }^{\circ}\text{C}$. It is seen that they form a marked segregation with concentration of Si increased by five times with respect to grain interior and its width constitutes several nanometers. Besides, grain boundary segregations of Mo, Cr and Si were detected in the steel produced by HPT at $400\text{ }^{\circ}\text{C}$ in

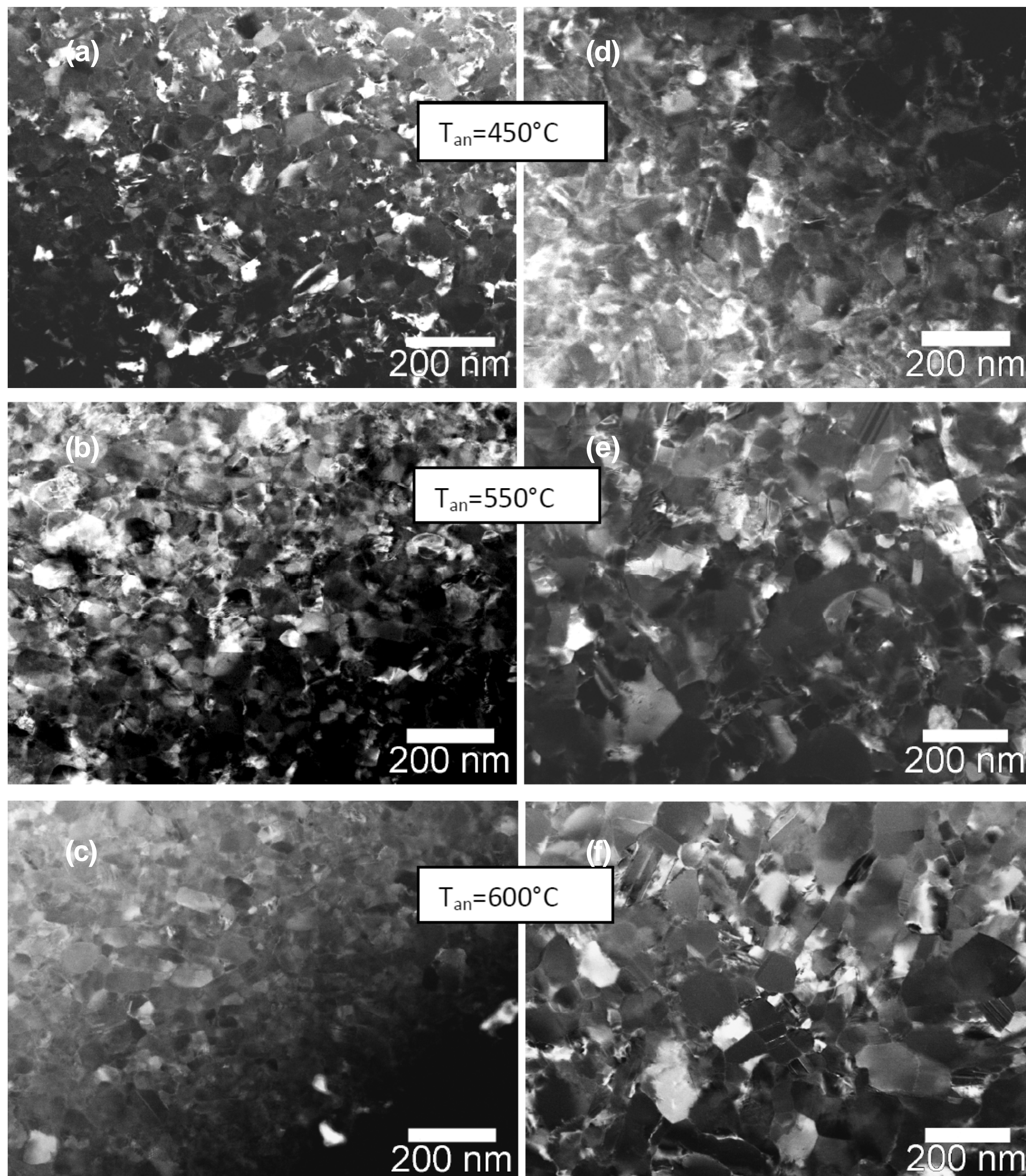


Fig. 3. STEM images of microstructure of an UFG austenitic stainless steel produced by HPT at room temperature (a-c) and at 400 °C (d-f) after 1 hour annealing at 450 °C (a,d), 550 °C (b,e), 600 °C (c,f).

agreement with [7] but not in the steel processed at room temperature as shown in [11].

The steel specimens in both UFG states were annealed for 1 hour in the temperature range from 450 °C to 700 °C. Upon annealing at 550 °C the microstructure exhibited no considerable changes. The grain size is relatively stable, grain boundaries became more straight and thinner while the dislocation density slightly decreased (Fig. 3). Annealing at 600 °C led to a slight increase of the grain size: ~65 nm and ~100 nm after HPT at room temperature and 400 °C, respectively. Annealing at 700 °C led to secondary recrystallization and notable grain growth for the case of the steel HPT-processed both at room temperature (up to the size of the biggest grains ~120 nm) [12] and at the elevated one (up to ~500 nm) – as displayed in Fig. 4a. As it was shown earlier [12] for the UFG steel produced by HPT at room temperature typical M_6C , $M_{23}C_6$, and

MC carbides were observed precipitated mostly in grain interior after annealing at 700 °C for 30 minutes. Similar effect took place for the UFG steel produced at elevated temperature after annealing at 700 °C for 10 minutes (Fig. 4a). Here, grain growth was followed by the formation of precipitates inside grains (Fig. 4a) as well as at grain boundaries (Fig. 4b). STEM-EDS analysis of the latter showed that they contained Mo, Cr and Si (Figs. 5a and 5b). Interestingly, the chemical composition of the precipitates corresponded to that of grain boundary segregations formed after HPT at elevated temperature.

Fig. 6 displays the results of microhardness measurements as a function of annealing temperature. It is seen that despite differences in grain size, both HPT-processed states demonstrate a similar level of hardness (590 ± 16 Hv) which exceeds by more than three times the value of the initial

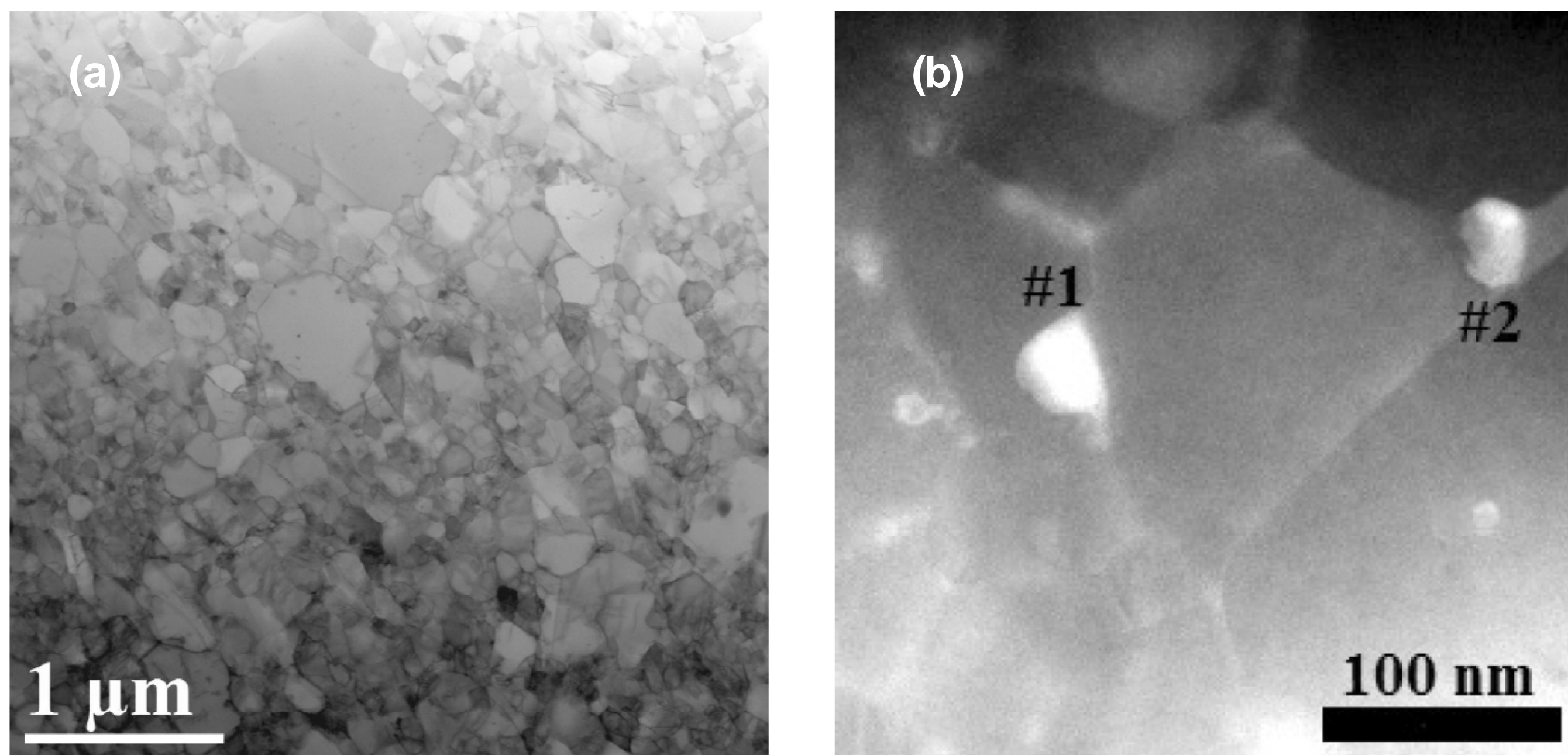


Fig. 4. STEM microstructure of the UFG steel produced by HPT at 400 °C after annealing at 700 °C for 10 min showing grain growth and formation of precipitates inside grains (a) and at grain boundaries (b).

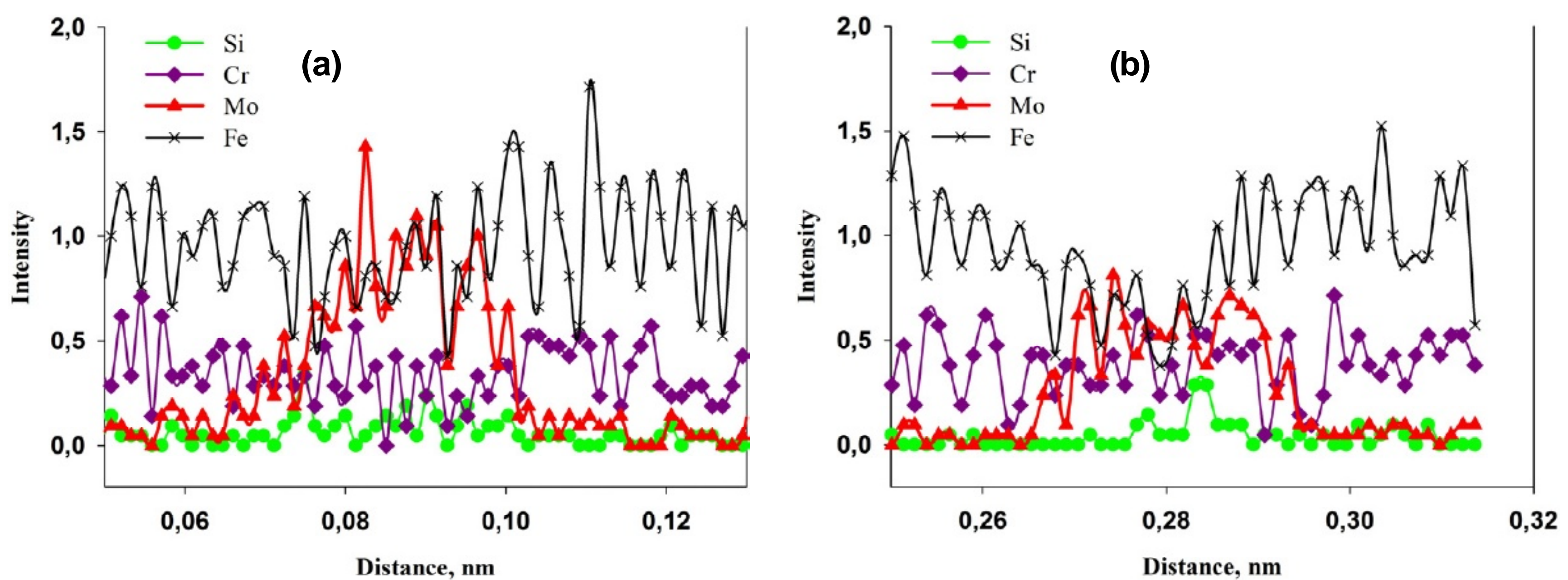


Fig. 5. STEM-EDS intensity profiles across precipitates from Fig. 4b #1(a) and #2 (b) in the austenitic stainless steel after HPT at 400 °C and annealing at 700 °C for 10 min revealing their Mo-Cr-Si composition.

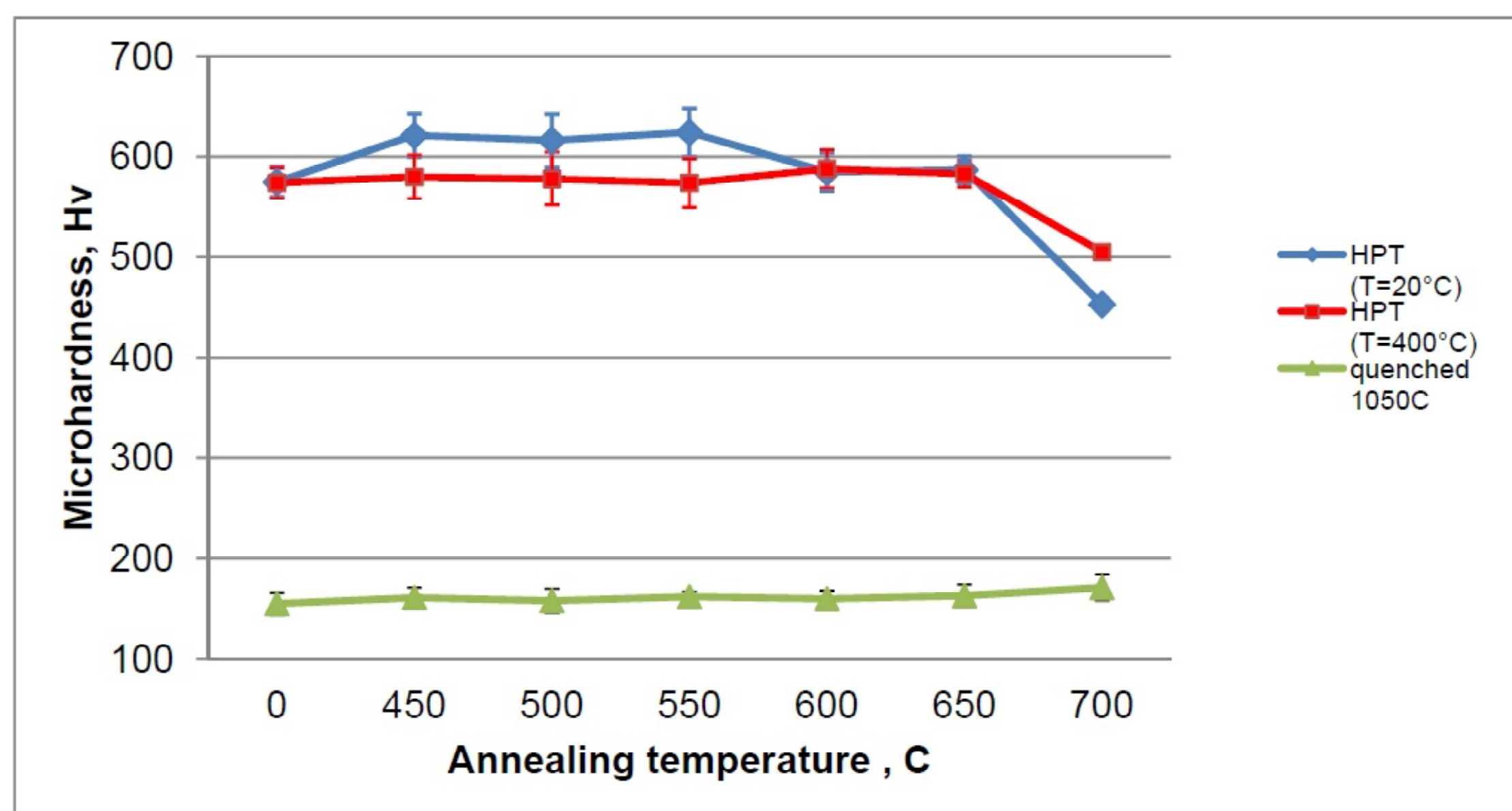


Fig. 6. Microhardness after 1 hour annealing at different temperatures.

quenched state (155 ± 11 Hv). Annealing in the temperature range from 450 °C to 550 °C of the UFG steel produced by HPT at room temperature slightly increased the hardness with a maximum at 550 °C ($\sim 630 \pm 20$ Hv), followed by a decrease from 550 °C to 650 °C. At the same time, the hardness of the UFG steel processed at 400 °C remained unchanged at annealing from 450 °C to 650 °C. A notable de-

crease in hardness was observed for the both UFG states after annealing at 700 °C, and this change was more pronounced for the case of the UFG steel produced by HPT at room temperature.

These results on the thermal stability of the UFG austenitic stainless steel produced by HPT at room temperature are in general consistent with the results reported in [8,9] where an increase of strength

with annealing after HPT at room temperature was reported. The difference with the current study is that the hardness level in the as-processed state was considerably lower in the cited references and increase in hardness/strength due to annealing was found to be much more elevated [8,9]. Wang et al. [9] explained this phenomenon by an elevation of the concentration of impurity at grain boundary regions due to annealing (they observed formation of G-phase at grain boundaries after long-term annealing). Alternatively, Renk et al. [8] explained the increase of strength by re-arrangement and annihilation of dislocations making the grain boundaries more resistant to thermally-induced migration. Besides, these authors [8] also reported the formation of grain boundary segregations in the UFG steel produced by HPT at room temperature due to annealing.

The presented results on different UFG states produced by HPT at different temperatures could be interpreted taking into account the following abovementioned findings: (i) for the UFG steel produced at room temperature there is no grain boundary segregation in the as-processed state, they appear after annealing at least at 550 °C [8]. With annealing, the hardness slightly grows while the defect density is reduced and the grain size remains unchanged or slightly increases starting from annealing at 600 °C; (ii) in the UFG steel produced by HPT at 400 °C the hardness level in the as-processed state is the same as for the HPT-processed steel at room temperature despite a notable difference in grain size. The grain boundary segregations are observed immediately after HPT at 400 °C. During annealing no notable change in hardness is observed until recrystallization starts. One could interpret unusual increase of hardness of room temperature HPT-processed steel as an indication of a considerable strengthening effect of grain boundary segregations forming due to thermal exposure. For the steel HPT-processed at 400 °C the segregations are already present in the as-processed state and they do not lead to additional hardening with annealing. At the same time in both UFG states the segregations can be responsible for the outstanding thermal stability (up to 650 °C) of the materials' strength – they could reduce the mobility of grain boundaries or the driving force for coarsening (by reducing the interfacial energy). After annealing at 700 °C, a higher value of hardness of the UFG steel produced by HPT at 400 °C as compared to the room temperature one was reported. It might be explained by an additional strengthening effect of

the observed Mo-Cr-Si precipitates which were not observed in the similar steel HPT-processed at room temperature and annealed at the same 700 °C [12].

4. SUMMARY

Two UFG states of an austenite stainless steel were produced by HPT at different temperatures. These states were characterized by different nanostructural features as grain size, defect density, and the presence of grain boundary segregations. As a result, these UFG states demonstrated different thermal behavior: we observed an increase of the hardness of UFG steel produced by HPT at room temperature after annealing up to 650 °C with maximum at 550 °C, while the hardness of UFG steel produced by HPT at 400 °C remained unchanged. Both states kept initial hardness level until annealing at 650 °C. At 700 °C a decrease in hardness was observed for both states associated with the onset of recrystallization processes. At that the hardness of the UFG steel produced by HPT at 400 °C exhibited higher redundant hardness value after 700 °C annealing than the room temperature HPT-processed steel. This observation can be linked with hardening effect of Mo-Cr-Si precipitates formed in the UFG steel processed at 400°C due to annealing at this temperature.

ACKNOWLEDGEMENTS

The authors acknowledge the financial support by the Russian Ministry of Science and Education under grant agreement No. 14.583.21.0012 (unique identification number RFMEFI58315X0012). A part of microstructure studies was conducted using the equipment of the Research Park of St. Petersburg State University at the Nanotechnology Center.

REFERENCES

- [1] R.Z Valiev, R.K. Islamgaliev and I.V. Alexandrov // *Prog. Mater. Sci.* **45** (2000) 103.
- [2] T.G. Langdon // *Acta Mater.* **61** (19) (2013) 7035.
- [3] A.P. Zhilyaev // *Prog. Mater. Sci.* **53** (2008) 893.
- [4] I. Shakhova // *Mat. Sci. Eng. A.* **545** (2012) 176.
- [5] R.S. Mishra, V.V. Stolyarov, C. Echer, R.Z. Valiev and A.K. Mukherjee // *Mat. Sci. Eng. A* **298** (2001) 44.
- [6] R.Z. Valiev, N.A. Enikeev and T.G. Langdon // *Kovove Mater.* **49** (2011) 1.

- [7] M.M. Abramova, N.A. Enikeev, R.Z. Valiev, A. Etienne, B. Radiguet, Y. Ivanisenko and X. Sauvage // *Mater. Letters* **136** (2014) 349.
- [8] O. Renk, A. Hohenwarter, K. Eder, K.S. Kormout, J.M. Cairney and R. Pippan // *Scripta Mater.* **95** (2015) 27.
- [9] H. Wang, I. Shuro, M. Umemoto, H.H. Kuo and Y. Todaka // *Mater Sci Eng A* **556:906** (2012) 10.
- [10] M.K. Miller, *Atom Probe Tomography: Analysis at the Atomic Level* (Springer, 2000).
- [11] A. Etienne, B. Radiguet, P. Pareige, J.-P. Massoud and C. Pokor // *J. Nuclear Mater.* **382** (2008) 64.
- [12] A. Etienne, B. Radiguet, C. Genevois, J.-M. Le Breton, R. Valiev and P. Pareige // *Mat. Sci. Eng. A* **527** (2010) 5805.